Journal of Environmental Management 202 (2017) 524–531

Contents lists available at ScienceDirect

Journal of Environmental Management

journal homepage: www.elsevier.com/locate/jenvman

Research article

The evolution of crop cultivation and paleoenvironment in the Longji Terraces, southern China: Organic geochemical evidence from paleosols

Yongjian Jiang [a], Shijie Li [b, c, *], Wei Chen [d], Desuo Cai [e], Yan Liu [f]

[a] College of Resources and Environment, Linyi University, Shuangling Road, Linyi 276000, PR China
[b] Institute of Geochemistry, Chinese Academy of Sciences, 99 West Lincheng Road, Guiyang 550081, PR China
[c] State Key Laboratory of Lake Science and Environment, Nanjing Institute of Geography and Limnology, Chinese Academy of Sciences, 73 East Beijing Road, Nanjing 210008, PR China
[d] Nanjing Institute of Geology and Palaeontology, Chinese Academy of Sciences, 39 East Beijing Road, Nanjing 210008, PR China
[e] College of Civil Engineering and Architecture, Guangxi University, 100 East Daxue Road, Nanning 530004, PR China
[f] Guangxi College of Water Resources and Electric Power, 99 Changgang Road, Nanning 530023, PR China

ARTICLE INFO

Article history:
Received 6 May 2016
Received in revised form
30 October 2016
Accepted 6 November 2016
Available online 15 November 2016

Keywords:
Ancient agricultural terraces
Organic geochemistry
Crop cultivation
Human-environment interaction
Southern China

ABSTRACT

The Longji ancient agricultural terraces in the Longji Mountain area (Guilin, southern China), which still remain in use, are famous for their magnificent terraced landscape with a mix of ecosystem and human inhabitation. Previous research has revealed the genesis and preliminary paleoenvironmental record of the agricultural terraces, but little is known about variations in crop cultivation over time. In this study, organic geochemical analyses and radiocarbon dating of an aggradational cultivated soil from a terrace profile were used to explore crop type variation and relevant paleoenvironmental change during the period of cultivation on the Longji Terraces. Hydroponic farming with rice (C_3) planting has been the dominant cultivation mode since the initial construction of the terraces. Warm-dry climate contributed to the growth of drought-tolerant crop (C_4) cultivation in the late 15th century. Temperature deterioration during the Little Ice Age had a negative impact on dry and hydroponic farming activities from the late 15th century to the late 19th century, while climate warming after the Little Ice Age promoted the redevelopment of hydroponic farming.

© 2016 Elsevier Ltd. All rights reserved.

1. Introduction

As common agricultural landscape features in mountainous areas worldwide, agricultural terraces present an ingenious way of transforming the original slope land into cultivable land. Ancient agricultural terraces, which were constructed in the historical period, may record abundant and insightful information about human-environment interaction in the past. Although there are differences in the environmental background, pattern, and type of cultivation between ancient agricultural terraces in different regions of the world, a range of common issues have been reported in previous studies. These include: (1) structure of terraced land and construction technology of the agricultural terraces (Ackermann et al., 2008; Beckers et al., 2013; Borisov et al., 2015; Gadot et al., 2016; Puy and Balbo, 2013); (2) exploring the genesis age or formation history of the terraces by radiocarbon dating or optically stimulated luminescence (OSL) dating (Beckers et al., 2013; Branch et al., 2007; Gadot et al., 2016; Henck et al., 2010; Jiang et al., 2014; Puy and Balbo, 2013); (3) natural environment and societal factors during the period of terrace formation (Boixadera et al., 2016; Gadot et al., 2016; Jiang et al., 2014; Puy and Balbo, 2013); and (4) evolution of farming activity during the historical periods recorded by the terraces (Ferro-Vázquez et al., 2014; Jiang et al., 2014; Trombold and Israde-Alcantara, 2005).

The Longji Terraces, located in Longsheng County of Guilin City in Guangxi Autonomous Region (Fig. 1), are one of the most famous ancient agricultural terraces in southern China. The terraces were built in historical periods by people of national minorities for habitation and cultivation in the Longji Mountain area. After a long-term development, the Longji Terraces area has formed a huge terrace system which is still in use for agriculture. Therefore, the

* Corresponding author. Institute of Geochemistry, Chinese Academy of Sciences, 99 West Lincheng Road, Guiyang 550081, PR China.
E-mail addresses: lishijie@vip.gyig.ac.cn, shjli@niglas.ac.cn (S. Li).

http://dx.doi.org/10.1016/j.jenvman.2016.11.016
0301-4797/© 2016 Elsevier Ltd. All rights reserved.

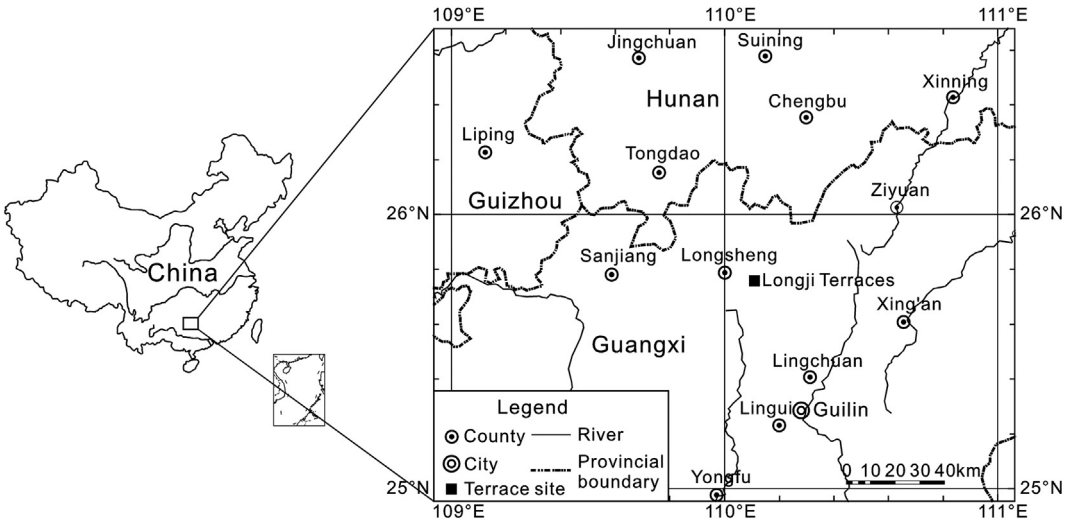

Fig. 1. Longji Terraces location map (after Jiang et al., 2014).

Longji Terraces provide materials for studies on the past human-environment interaction as well as the protection and management of the terrace system. However, research on historical paleoenvironmental change and human activity in Chinese ancient terraces is limited. Previous work by the present authors has revealed the origin and historical background of the Longji Terraces, and also provided preliminary findings on variations in the intensity of farming activity and environmental changes over the past few hundred years based on radiocarbon dating, and physical and geochemical analyses of selected soil profiles (Jiang et al., 2014).

In order to further explore historical human-environment interaction in the Longji Terraces area, in this study we implement analysis of *n*-alkanes and organic carbon stable isotopes ($\delta^{13}C_{org}$) in cultivated soil. The lipoid *n*-alkanes are some of the most studied biomarkers because of their stability in geological materials (Xie et al., 2003). When preserved in geological materials, *n*-alkane distributions reflect the original organic material and have been shown to react to climate and environmental change sensitively. Accordingly, *n*-alkanes have been used to identify the source of organic matter, paleovegetation, and paleoenvironmental evolution (Zheng et al., 2005). A range of studies have inferred paleoenvironmental factors from *n*-alkane evidence in various materials, such as lacustrine sediment (Cao et al., 2016; Pu et al., 2011; van Bree et al., 2014), marine sediment (Badejo et al., 2016; Badewien et al., 2015; Ratnayake et al., 2006), loess–paleosol sequences (Schäfer et al., 2016; Zech et al., 2012; Zhang et al., 2006), and archaeological strata (Gupta et al., 2013; Zou et al., 2007). Another widely utilized organic geochemical proxy in paleoenvironmental research is the carbon isotope $\delta^{13}C_{org}$. Analysis of $\delta^{13}C_{org}$ in loess–paleosol sequences (Dar et al., 2015; Liu et al., 2005; Rao et al., 2013) has been used to estimate the relative abundance of C_3 and C_4 plants in the past, for reconstruction of paleovegetation and its paleoclimatic significance. In studies of lacustrine sediment (Gałka and Apolinarska, 2014; O'Beirne et al., 2015; Selvaraj et al., 2012), $\delta^{13}C_{org}$ combined with TOC/TN (total organic carbon/total nitrogen) has been found to be an effective indicator of organic matter source, and the evolution of lake environment and paleoclimate. In archaeological strata, $\delta^{13}C_{org}$ has also been used to identify relationships between paleoenvironmental change and human activity (Huckleberry and Fadem, 2007; Parker et al., 2011).

In agricultural terraces, abundant organic matter has been left in the soil during the crop cultivation, which provides ideal material to reveal information about historical crop cultivation by the analyses of *n*-alkanes and $\delta^{13}C_{org}$. However, application of *n*-alkanes and $\delta^{13}C_{org}$ in research on ancient terraces has not been widely reported. Here, we analyze *n*-alkanes and $\delta^{13}C_{org}$ from cultivated soil in the Longji agricultural terraces, in combination with results from previous radiocarbon dating and TOC analysis (Jiang et al., 2014), to investigate variations in crop type associated with historic paleoenvironmental change since the terraces were constructed. The sustainability of the grand scale and good preservation of the Longji Terraces requires effective management of the mix of ecosystem and human inhabitation. In this study, exploring information on the past evolution of cultivation in the terraces may reveal the changes of crop cultivation caused by paleoclimatic variation as well as the predominant cultivation mode during the development history of the Longji Terraces. This information is expected to give some helpful indicators for how to keep the sustainable and effective preservation of the terrace system and how to adjust the crop cultivation with environmental difference, which is meaningful for long-term management of the terrace landscape.

2. Study area

The Longji Terraces are distributed over the Longji Mountain area, west of Yuechengling Mountain. The Longji Mountain area (300–1850 m asl) is characterized by an integrated geomorphologic landscape of high mountains, river terraces, and river valleys which have developed under the impact of tectonic movements in geological periods (Cheng et al., 2002). The main parent rocks are metamorphics of the Banxi Group, Upper Proterozoic Jixian System, which date back 800 million years (Tong, 2006). Mid-subtropical monsoon climate with the influence of altitude is prevalent in the Longji Terraces area, with annual average temperature of 14.4–16.9 °C and annual precipitation of 1600–1733 mm (Cheng et al., 2002).

Ping'an village (Fig. 2a), in the core of the Longji Terraces area, was selected as the study site for fieldwork and sampling. The terraces around Ping'an village (Fig. 2b and c) are generally considered as the initial settlement of the ancients, and provide a good representation of the study area. Ping'an village terraces consist of more than 15,000 blocks of large and small agricultural terraces, with a maximum altitude of 880 m, a minimum of 380 m, and an area of 4 km^2. The main food crop cultivated on the terraces is rice.

Fig. 2. (a) Ping'an village in the Longji Terraces area; (b, c) Agricultural terraces around Ping'an village; (d) Gravity irrigation through Longji agricultural terraces (a, b and d after Jiang et al., 2014).

Longji agricultural terraces are commonly constructed parallel to hillslope contours, on slopes of 26–35° (Cheng et al., 2002), and are composed of flat treads (cultivated areas), terrace walls (risers), and field ridges on top of the walls (Fig. 2d). A gravity irrigation system is implemented; irrigation water flows downwards from a water source in a higher altitude area, through natural watercourses and anthropogenic channels or pipes (Fig. 2d), to irrigate the terraces. The local inhabitants maintain and heighten the field ridges periodically.

3. Materials and methods

One soil profile (LJTT-3), located close to inhabited area in Ping'an village was chosen for detailed study considering that the terrace containing profile LJTT-3 was probably one of the first to be developed for its adjacency to the inhabited area. The altitude and coordinates of the profile are 800 m asl and 25° 45.4061′ N, 110° 6.99′ E, respectively (see Fig. 3). Profile description was carried out following the USDA system of soil classification, as introduced by Xi (1994). LJTT-3 consists of the modern cultivated soil horizon (Ap), buried cultivated soil horizons (Abp1 and Abp2), with Bw, B/C and C horizons below, although bedrock was not reached. The long sequence of cultivated horizon makes LJTT-3 appropriate for this study. Aggradational features have been identified in the cultivated horizon of LJTT-3, which are thought to be associated with the gravity irrigation system and annual heightening of the field ridges (Jiang et al., 2014).

A total of 74 samples were taken from profile LJTT-3, including 70 at intervals of 1 cm between 0 and 70 cm depth, and 4 extracted with regard to the degree of weathering between 70 and 85 cm depth. In addition, one paleosol sample (LJTT-4-C) was collected for radiocarbon dating from the bottom of the cultivated horizon in an adjacent, similar profile (LJTT-4).

Analysis of *n*-alkanes was performed with a 6890N gas chromatograph (Agilent Technologies) at the Key Laboratory of Marginal Sea Geology, Guangzhou Institute of Geochemistry, Chinese

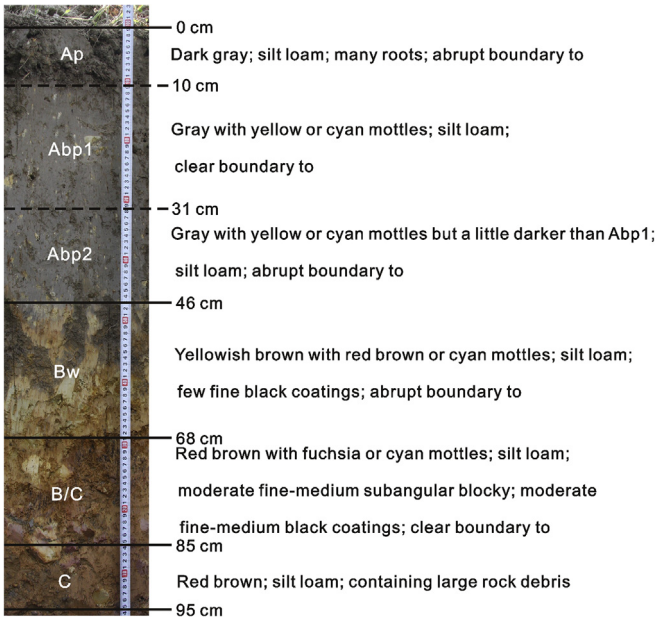

Fig. 3. Field description of profile LJTT-3 from Ping'an village (after Jiang et al., 2014).

Academy of Sciences. A 2–3 g sample of dried and powdered soil was ultrasonically extracted with dichloromethane three times. The combined solvents were concentrated using a rotary evaporator. The total lipid extract was separated by silica gel flash-column chromatography using n-hexane in order to obtain the saturated hydrocarbon fraction. Then the samples were treated by the urea complexation method, using n-hexane as the extraction agent for final analysis. The chromatograph is equipped with an HP-1 silica capillary column (30 m × 0.25 mm × 0.25 μm). The oven temperature program was as follows: 80 °C for 2 min; increasing to

140 °C at a rate of 10 °C/min; then increasing to 300 °C at a rate of 6 °C/min; and maintaining at 300 °C for 15 min. The carrier gas was nitrogen and the sample injection volume was 1 μL.

Organic carbon stable isotope ($\delta^{13}C_{org}$) analysis was performed with a DELTA^{plus} Advantage stable isotope mass spectrometer at the State Key Laboratory of Lake Science and Environment, Nanjing Institute of Geography and Limnology, Chinese Academy of Sciences. Sample pretreatment included: (1) heating in a water-bath and using HCl solution to remove inorganic carbon; (2) using deionized water to rinse the sample until it had a neutral pH; (3) drying and grinding.

AMS ^{14}C dating of five soil samples from different depths in the cultivated horizon of profile LJTT-3, and of sample LJTT-4-C, was performed at the Accelerator Mass Spectrometry Laboratory of Peking University. Radiocarbon ages were calibrated by the OxCal V4.1.7 program (Bronk Ramsey, 2009) and the IntCal09 calibration curve (Reimer et al., 2009). Weighted averaging of ages at 2σ precision was used to determine the calibrated ages.

4. Results and discussion

4.1. Radiocarbon dating results

Table 1 shows the radiocarbon dating ages and calibrated calendar ages of samples from Ap, Abp1, and Abp2 horizons of profile LJTT-3, and sample LJTT-4-C. In the cultivated horizon of LJTT-3, sample ages increase with depth, which confirms that it is an aggradational sequence, and means that the basal age of the horizon should be a good indicator of when cultivation was initiated (Jiang et al., 2014).

Paleosol sample LJTT-3-5-C revealed a ^{14}C age of 545 ± 30 yr BP and a calibrated age of 1361–1406 yr AD, which are very similar to the ages of paleosol sample LJTT-4-C (575 ± 25 yr BP, 1335–1384 yr AD); these ages correspond to the late period of the Yuan Dynasty in Chinese history. The two paleosol samples were taken from the base of the cultivated horizon in profiles LJTT-3 and LJTT-4, which are two adjacent and parallel profiles, with similar cultivated horizon thicknesses. Therefore, the ages suggest that initial formation of the cultivated horizon on the terraces dates back to the late Yuan Dynasty, which is a good indicator for the origin of Longji Terraces (Jiang et al., 2014).

4.2. n-alkanes

The carbon numbers of *n*-alkanes were determined according to retention time in the GC (gas chromatography) chromatogram. The relative abundance of *n*-alkanes (RA_i), calculated based on area beneath *n*-alkane peaks in the GC chromatogram, is defined as follows,

$$RA_i = P_i \Big/ \sum P_i \quad (1)$$

where P_i is the peak area of *n*-alkane with a carbon number of *i*, and $\sum P_i$ is the total area of all *n*-alkanes.

The carbon numbers of *n*-alkanes extracted from the cultivated soil samples of profile LJTT-3 range from 14 to 35, and show unimodal or bimodal distribution (Fig. 4). In samples with a unimodal distribution pattern, *n*-C_{29}, *n*-C_{31}, and *n*-C_{33} are the predominant *n*-alkanes, with the maximum at *n*-C_{31} in the long-chain component. In samples with a bimodal distribution pattern, *n*-C_{15}, *n*-C_{16}, *n*-C_{17}, and *n*-C_{18} are predominant in the short-chain component, with maximum *n*-C_{16}, and *n*-C_{29}, *n*-C_{31}, and *n*-C_{33} are predominant in the long-chain component, with the maximum at *n*-C_{31}. Long-chain *n*-alkanes present higher relative abundance than short-chain *n*-alkanes in most bimodal distribution samples. All samples show evident odd-over-even preference in long-chain *n*-alkanes, while no obvious odd/even predominance in short-chain *n*-alkanes. It has been suggested that *n*-alkanes with different chain lengths indicate different sources of organic matter. Those derived from lower organisms such as photosynthetic bacteria and algae are mainly short-chain *n*-alkanes (<*n*-C_{21}), dominated by *n*-C_{17}, *n*-C_{18}, or *n*-C_{19}, with no obvious odd-over-even preference (Cranwell et al., 1987; Gelpi et al., 1970). Submerged and floating plants and mosses mainly produce middle-chain *n*-alkanes dominated by *n*-C_{21}, *n*-C_{23}, or *n*-C_{25} (Corrigan et al., 1973; Ficken et al., 2000), while *n*-alkanes derived from terrestrial higher plants are mainly long-chain *n*-alkanes with significant odd-over-even preference, and dominated by *n*-C_{27}, *n*-C_{29}, or *n*-C_{31} (Eglinton and Hamilton, 1967). Therefore, we conclude that *n*-alkanes extracted from the cultivated soil of profile LJTT-3 were mainly derived from terrestrial higher plants, supplemented by some derived from lower organisms.

The ratio of relative abundance of high-carbon-number *n*-alkanes (≥C_{21}) to low-carbon-number *n*-alkanes (≤C_{20}) (RA_H/RA_L) was calculated as follows,

$$RA_H/RA_L = \sum_{i=21}^{m} RA_i \Big/ \sum_{j=14}^{n} RA_j \quad (2)$$

where RA_i and RA_j are the relative abundance of *n*-alkane with a carbon number of *i* and a carbon number of *j* respectively, and $m = 35$, $n = 20$. The calculated results for profile LJTT-3 show that RA_H/RA_L values range from 1.28 to 13.84, with a mean value of 4.09 (Fig. 5e), reflecting the higher relative abundance of high-carbon-number *n*-alkanes, indicative of terrestrial higher plants.

Woody terrestrial higher plants mainly produce *n*-alkanes dominated by *n*-C_{27} or *n*-C_{29}, while herbaceous plants mainly produce *n*-alkanes dominated by *n*-C_{31} or *n*-C_{33} (Cranwell, 1973). Long-chain *n*-alkanes in the cultivated soil of profile LJTT-3 generally show relative abundance of *n*-C_{31}>*n*-C_{33}>*n*-C_{29}>*n*-C_{27}, suggesting a greater contribution of herbaceous plants than woody plants, which supports a crop residue origin of organic matter in the cultivated horizon. The ratio of *n*-alkanes from herbaceous plants to woody plants, (C_{31}+C_{33})/(C_{27}+C_{29}) was calculated as follows,

Table 1
Radiocarbon dating results of soil samples from Longji Terraces (after Jiang et al., 2014).

Profile	Sample no.	Lab no.	Depth (cm)	Material	^{14}C age (yr BP)	Calibrated age (2σ) (yr AD)
LJTT-3	LJTT-3-1-C	BA101723	9–10	Organic matter	Modern carbon±25	
	LJTT-3-2-C	BA101724	18–19	Organic matter	25 ± 25	1846–1883
	LJTT-3-3-C	BA120408	28–29	Organic matter	430 ± 25	1428–1491
	LJTT-3-4-C	BA120409	32–33	Organic matter	440 ± 25	1422–1481
	LJTT-3-5-C	BA101721	44–45	Organic matter	545 ± 30	1361–1406
LJTT-4	LJTT-4-C	BA101722	45–46	Organic matter	575 ± 25	1335–1384

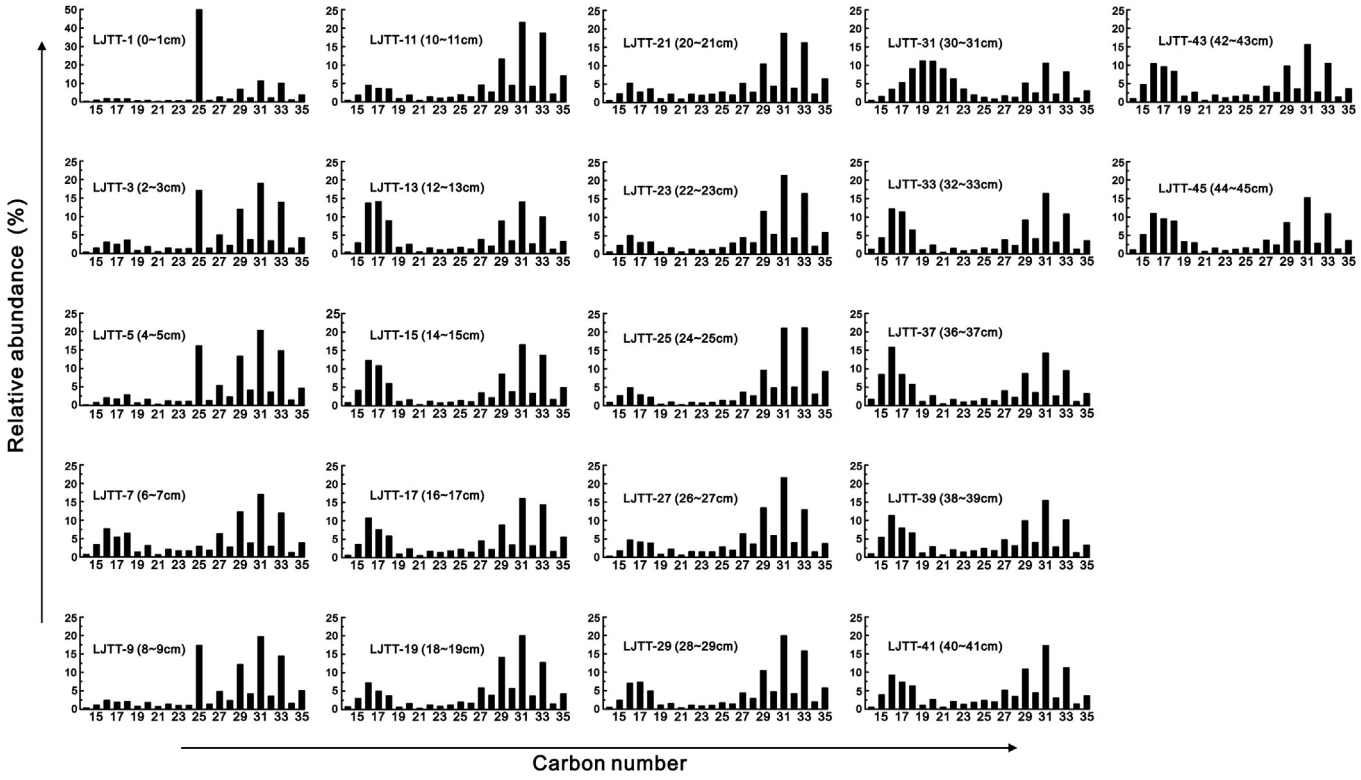

Fig. 4. Distribution of *n*-alkane in the cultivated horizon of profile LJTT-3.

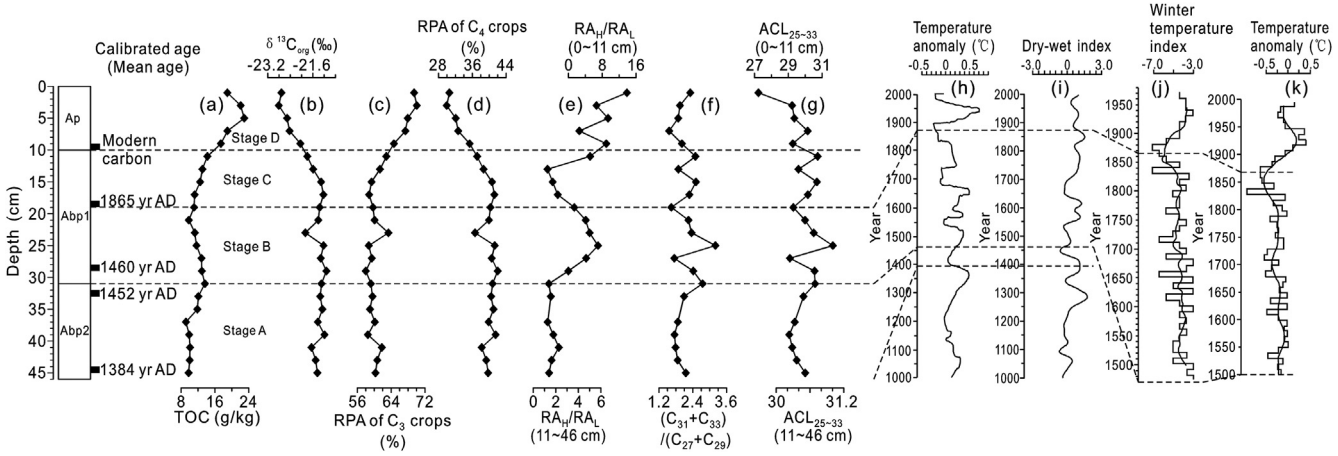

Fig. 5. Multiple proxy results. (a)–(g) Organic geochemical proxies for the cultivated horizon of profile LJTT-3. Calibrated ages and total organic carbon (TOC) variation are derived from Jiang et al. (2014); (h) South China temperature anomaly, 1000–2000 AD (after Wang, 2007); (i) standardized annual dry-wet index, 1000–2000 AD, for Jiang-Nan area, China, using 30-year fast Fourier transformation (FFT) filter smoothing (after Zheng et al., 2006); (j) winter temperature index from the 1470s–1970s for Guangdong and Guangxi, China, based on 50-year moving average (after Zhang, 1980); (k) South China annual temperature anomaly, based on 10-year averages, 1500–2000 AD (after Wang et al., 1998).

$$(C_{31}+C_{33})/(C_{27}+C_{29}) = (RA_{31}+RA_{33})/(RA_{27}+RA_{29}) \quad (3)$$

where RA_{31}, RA_{33}, RA_{27} and RA_{29} correspond to the relative abundance of *n*-C_{31}, *n*-C_{33}, *n*-C_{27}, and *n*-C_{29}, respectively. Calculated values of $(C_{31}+C_{33})/(C_{27}+C_{29})$ in profile LJTT-3 range from 1.56 to 3.20, with a mean value of 2.13 (Fig. 5f), indicating the higher relative abundance of *n*-C_{31} and *n*-C_{33}, which again reflects the predominance of *n*-alkanes from herbaceous plants.

Considering the relatively high concentrations of *n*-C_{25} to *n*-C_{33} in the cultivated horizon of profile LJTT-3, the average chain length (ACL) of odd-carbon-number *n*-alkanes ranging from *n*-C_{25} to *n*-C_{33} was calculated as follows,

$$ACL_{25-33} = (25\times RA_{25} + 27\times RA_{27} + 29\times RA_{29} + 31\times RA_{31} + 33\times RA_{33})/(RA_{25}+RA_{27}+RA_{29}+RA_{31}+RA_{33}) \quad (4)$$

where RA_{25}, RA_{27}, RA_{29}, RA_{31}, and RA_{33} correspond to the relative abundance of *n*-C_{25}, *n*-C_{27}, *n*-C_{29}, *n*-C_{31}, and *n*-C_{33}, respectively. Calculated ACL_{25-33} values in profile LJTT-3 range from 27.23 to 31.01, with a mean value of 30.18 (Fig. 5g). Correlation analysis of

samples in the Abp1 and Abp2 horizons shows a significant positive correlation between ACL_{25-33} and $(C_{31}+C_{33})/(C_{27}+C_{29})$ ($Y = 0.5X+29.42$, Y is ACL_{25-33}, X is $(C_{31}+C_{33})/(C_{27}+C_{29})$, $R^2 = 0.94$, $P < 0.001$). This suggests that when crop planting increased, *n*-alkanes from herbaceous plants became more abundant in the cultivated soil, with higher $(C_{31}+C_{33})/(C_{27}+C_{29})$, correspondingly, ACL_{25-33} increased. Moreover, when crop planting reduced, *n*-alkanes from herbaceous plants became less abundant in the cultivated soil, with lower $(C_{31}+C_{33})/(C_{27}+C_{29})$, and ACL_{25-33} also decreased.

4.3. Organic carbon stable isotopes

Terrestrial plants can be divided into C_3, C_4, and CAM (crassulacean acid metabolism) plants according to different mechanisms of photosynthesis (Bowen, 1991). C_3 plants include woody, and most herbaceous and shrub plants, C_4 plants include some herbaceous and shrub plants (Deines, 1980; Farquhar et al., 1989). CAM plants mainly include desert succulents, and epiphytes in tropical rain forests (Osmond, 1978). $\delta^{13}C_{org}$ values of C_3 plants range from −20‰ to −34‰, with a mean value of −27‰, and $\delta^{13}C_{org}$ values of C_4 plants range from −9‰ to −19‰, with a mean value of −13‰ (Deines, 1980; Farquhar et al., 1989).

Organic matter in the cultivated horizon of profile LJTT-3 was mainly derived from crop residues. Rice cultivation prevails in the Longji Terraces, and rice is a C_3 plant with $\delta^{13}C_{org}$ value around −28.5‰ (Ci et al., 2007). In this study, mean $\delta^{13}C_{org}$ values of modern plants (−27‰ and −13‰) were used as endpoints to estimate the relative plant abundance (RPA) of C_3 and C_4 plants. Specifically, $\delta^{13}C_{org}$ values greater than −13‰ indicate pure C_4 vegetation (0% relative abundance of C_3 plants); $\delta^{13}C_{org}$ values less than −27‰ indicate pure C_3 vegetation (0% relative abundance of C_4 plants); $\delta^{13}C_{org}$ values between −13‰ and −27‰ reflect mixed vegetation of C_3 and C_4 plants.

Results show that $\delta^{13}C_{org}$ values for the cultivated horizon in profile LJTT-3 range from −22.81‰ to −21.12‰, with a mean value of −21.64‰ (Fig. 5b), which shows co-contribution of C_3 and C_4 plants to the composition of the organic carbon isotope, indicative of C_3/C_4 mixed vegetation. The RPA of C_3 plants ranged from 58% to 70.07%, with a mean value of 61.75% (Fig. 5c), and of C_4 plants ranged from 29.93% to 42%, with a mean value of 38.25% (Fig. 5d). This suggests that the mode of cultivation during the development of Longji Terraces probably comprised a rotation of C_3 and C_4 crops, dominated by C_3 crops. C_3 crops such as rice are thermophilic and hygrophilous, while C_4 crops are more drought-tolerant (Liu et al., 2005; Rao et al., 2010; Ni et al., 2011). Therefore, variations in $\delta^{13}C_{org}$, and RPA of C_3 and C_4 crops, in the cultivated horizon of profile LJTT-3 may be used to indicate changes in crop cultivation associated with climatic fluctuations since initiation of the Longji Terraces.

4.4. Crop cultivation and environmental records of profile LJTT-3

From our previous work (Jiang et al., 2014), four soil development stages were distinguished in the cultivated horizon of profile LJTT-3: Stage A (46–31 cm), Stage B (31–19 cm), Stage C (19–10 cm), and Stage D (10–0 cm). In this study, we explored the evolution of crop cultivation and environment based on the organic geochemical evidence for each of the four stages.

4.4.1. Stage A (46–31 cm depth): late 14th century to late 15th century

In this stage, lower TOC, $(C_{31}+C_{33})/(C_{27}+C_{29})$, and ACL_{25-33} (Fig. 5a, f and g) indicate reduced crop cultivation. RA_H/RA_L is also lower (Fig. 5e), reflecting larger amounts of low-carbon-number *n*-alkanes, which might be derived from microorganisms, or caused by microbial degradation of *n*-alkanes from higher plants (Cui et al., 2008). Accordingly, relatively strong microorganism activity can be inferred during this stage. The anaerobic environment under hydroponic crop farming may constrain the decomposition of organic matter by microorganisms to some extent (Xi, 1994). Therefore, higher intensity of microbial activity might suggest weaker hydroponic farming activity in this stage.

Enhancement of farming activity may be inferred in the late period of Stage A, based on increased TOC content, $(C_{31}+C_{33})/(C_{27}+C_{29})$, and ACL_{25-33} (Fig. 5a, f and g). In addition, $\delta^{13}C_{org}$ becomes more positive, with a decline in RPA of C_3 crops and an increase in RPA of C_4 crops (Fig. 5b–d). This may reflect increased cultivation of drought-tolerant crops under dry and warm climate. RA_H/RA_L declines in the late period of Stage A (Fig. 5e), suggesting increased low-carbon-number *n*-alkanes, which might be caused by strong microbial activity under the warm-dry climate. The climate change at the end of Stage A seems to be related to the warming and drying climate in South China in the early to late 15th century (Fig. 5h and i).

4.4.2. Stage B (31–19 cm depth): late 15th century to late 19th century

Stage B displays higher TOC, $(C_{31}+C_{33})/(C_{27}+C_{29})$, and ACL_{25-33} than Stage A (Fig. 5a, f and g), reflecting greater input of organic matter and high-carbon-number *n*-alkanes from higher plants, especially herbaceous plants. This suggests a general enhancement of farming activity in Stage B compared with Stage A.

TOC content decreases from bottom to top within Stage B (Fig. 5a), suggestive of a weakening in farming activity over the period, which is also supported by the decline of $(C_{31}+C_{33})/(C_{27}+C_{29})$ and ACL_{25-33} in the late phase of Stage B (Fig. 5f and g). $\delta^{13}C_{org}$ becomes more negative in the late period of Stage B, with an increase in RPA of C_3 crops and a decrease in RPA of C_4 crops (Fig. 5b–d), which might reflect relatively cool and wet climate, leading to the weakening of dry farming activity. RA_H/RA_L abruptly declines in the late period of Stage B (Fig. 5e), which denotes a decrease in the relative abundance of high-carbon-number *n*-alkanes and an increase in low-carbon-number *n*-alkanes, suggesting a weakening of hydroponic farming activity. However, RA_H/RA_L values at the end of Stage B are much higher than in Stage A, indicating that hydroponic farming activity in the late period of Stage B was probably still stronger than that in Stage A. Therefore, it is inferred that the weakening of hydroponic farming activity at the end of Stage B was not caused by a drier climate, but was probably the result of a deterioration in temperature.

Previous research has suggested that climate cooling in South China after the 1480s indicated the start of the Little Ice Age (Ge et al., 2011). Other studies have revealed a fluctuating temperature decline in South China during the period corresponding to Stage B, with a particularly sharp drop after 1700 AD, and a relatively humid phase from 1700 AD to the 1860s (Fig. 5h–k). The paleoenvironmental record of a sediment core from Sihu Lake in Guilin, China, also revealed cold-wet climate from the early 18th century to the late 19th century (Li et al., 2009). Therefore, the weakening of farming activity within Stage B is likely to reflect the influence of the Little Ice Age temperature decline on the crop cultivation. The decrease in farming activity was especially significant in the late period of Stage B, suggesting this corresponded to the coldest phase of the Little Ice Age.

4.4.3. Stage C (19–10 cm depth): late 19th century to the modern period

Over this stage, TOC gradually increases (Fig. 5a), and $(C_{31}+C_{33})/(C_{27}+C_{29})$ and ACL_{25-33} show a more fluctuating increase (Fig. 5f

and g). This reflects greater input of organic matter with high-carbon-number *n*-alkanes from herbaceous plants, suggesting a gradual growth in crop cultivation. Also within Stage C, $\delta^{13}C_{org}$ gradually becomes more negative, RPA of C_3 crops increases, and RPA of C_4 crops decreases (Fig. 5b–d), which suggests enhancement of hydroponic farming activity as temperature levels improved. At the end of Stage C, RPA of C_3 crops increases, RPA of C_4 crops decreases (Fig. 5c and d), and RA_H/RA_L increases markedly (Fig. 5e), indicating a major increase in hydroponic farming activity.

According to other studies, temperature in South China began to rise significantly in late 19th century, after termination of the little Ice Age (Fig. 5h, j and k), and humidity was relatively high (Fig. 5i). As the mean calibrated age for the initiation of Stage C was 1865 AD, the enhancement of hydroponic farming activity after this was probably a response to the warmer and wetter climate. South China temperature peaked in the 1940s (Fig. 5h, j and k), during the warmest sub-period of the Modern Warm Period (Hansen et al., 2010; Wang and Tang, 2011), and rainfall was also relatively high (Wang et al., 2002). Therefore, the significant increase in hydroponic farming activity at the end of Stage C might be related to the warm and humid climate of the 1940s.

4.4.4. Stage D (10–0 cm depth): modern farming period

In this stage, much higher TOC content (Fig. 5a), and increasingly negative $\delta^{13}C_{org,}$ with RPA of C_3 crops increasing and of C_4 crops decreasing (Fig. 5b–d), reflect strong hydroponic farming activity during the modern warming period. A clear increase in RA_H/RA_L and decrease in ACL_{25-33} (Fig. 5e and g) is likely to be related to the high relative abundance of *n*-C_{25} in this soil layer (Fig. 4), which might indicate the contribution of *n*-alkanes from mosses. However, interpretation of the modern cultivated soil horizon is difficult, due to the complex influence of anthropogenic factors, such as modern fertilizer application, crop quality improvement, and creation of the terrace landscape.

5. Conclusions

The Longji ancient agricultural terraces in southern China, famous as a spectacular landscape, are still in use for large scale crop cultivation today. In previously published work, we have reported on the origin of the Longji Terraces, along with presentation of preliminary information on past human-environment interactions (Jiang et al., 2014). Here, building on our previous results, we further explored the evolution of crop cultivation and paleoenvironmental changes, from initiation of the terraces (1361–1406 yr AD) to the present, based on analyses of organic geochemical proxies.

Organic geochemical data from a selected terrace soil profile suggested that organic matter in the cultivated horizon was mainly derived from terrestrial herbaceous plants, including both C_3 and C_4 crops, but was dominated by C_3 crops. Four soil development stages were identified, and variations in the nature and intensity of crop cultivation with paleoclimatic change were examined for each stage. In the late 15th century, farming activity was enhanced with the growth drought-tolerant crop cultivation (C_4 crop) in a relatively warm and dry climate. The Little Ice Age affected the Longji Terraces area from the late 15th century to the late 19th century, with significant climate cooling. This seems to have been associated with weakening of both dry and hydroponic farming activities, particularly in the later part of this stage. After the termination of Little Ice Age in the late 19th century, climate warming commenced and hydroponic farming activity began to intensify. The enhancement of hydroponic farming activity in the modern farming period might be related to climate warming, although modern farming methods, and development of the ancient terrace landscape, were also contributing factors.

The extensive terrace system in the Longji area has been supporting intensive and productive cultivation for more than 600 years, and represents an integration of past technology and modern development. The historical relationship between crop cultivation and paleoenvironment discussed in this study may provide insights for current or future management of the terrace system in the Longji Terraces. Elaborate maintenance of the flat treads and field ridges during the process of hydroponic farming on the terrace, which can effectively prevent water loss and soil erosion, may contribute to the well conservation of the terrace system from its initial construction to now in the Longji Terraces area. The types of crop cultivation could be adjusted according to climate change or environmental difference at different altitudes so as to ensure that the cultivation adapts to environment, which is beneficial for the sustainable development of agriculture in the Longji Terraces area. In addition, in future work, construction of more extensive chronology and paleoenvironmental record will provide more detail on the agricultural development of the terraces, which may further contribute to their long-term management and that of the wider landscape.

Acknowledgements

This study was supported by an innovation project from Institute of Geochemistry, Chinese Academy of Sciences (Grant no. Y5CJ037000), Shandong Provincial Nature Science Foundation (grant no. ZR2015DL008) and Guangxi Provincial Water Resources Department (grant no. GTT201002). We thank local staff for support during the field work. We are especially indebted to Prof. Guodong Jia who provided great help in the *n*-alkane analysis. We would like to thank Editage [www.editage.cn] for English language editing. We are grateful to editors and two anonymous reviewers for their valuable suggestions.

References

Ackermann, O., Svoray, T., Haiman, M., 2008. Nari (Calcrete) outcrop contribution to ancient agricultural terraces in the Southern Shephelah, Israel: insights from digital terrain analysis and a geoarchaeological field survey. J. Archaeol. Sci. 35, 930–941.

Badejo, A.O., Choi, B.H., Cho, H.G., Yi, H.I., Shin, K.H., 2016. Environmental change in Yellow Sea during the last deglaciation to the early Holocene (15,000–8,000 BP). Quat. Int. 392, 112–124.

Badewien, T., Vogts, A., Dupont, L., Rullkötter, J., 2015. Influence of Late Pleistocene and Holocene climate on vegetation distributions in southwest Africa elucidated from sedimentary *n*-alkanes – differences between 12°S and 20°S. Quat. Sci. R 125, 160–171.

Beckers, B., Schütt, B., Tsukamoto, S., Frechen, M., 2013. Age determination of Petra's engineered landscape—optically stimulated luminescence (OSL) and radiocarbon ages of runoff terrace systems in the Eastern Highlands of Jordan. J. Archaeol. Sci. 40, 333–348.

Boixadera, J., Riera, S., Vila, S., Esteban, I., Albert, R.M., Llop, J.M., Poch, R.M., 2016. Buried A horizons in old bench terraces in Les Garrigues (Catalonia). Catena 137, 635–650.

Borisov, A.V., Chernysheva, E.V., Korobov, D.S., 2015. Buried paleoanthrosols of the bronze age agricultural terraces in the Kislovodsk basin (northern caucasus, Russia). Quat. Int. http://dx.doi.org/10.1016/j.quaint.2015.08.054.

Bowen, R., 1991. Isotopes and Climates. Elsevier Applied Science, London.

Branch, N.P., Kemp, R.A., Silva, B., Meddens, F.M., Williams, A., Kendall, A., Vivanco, C., 2007. Testing the sustainability and sensitivity to climatic change of terrace agricultural systems in the Peruvian Andes: a pilot study. J. Archaeol. Sci. 34, 1–9.

Bronk Ramsey, C., 2009. Bayesian analysis of radiocarbon dates. Radiocarbon 51, 337–360.

Cao, H.R., Hu, J.F., Peng, P.A., Xi, D.P., Tang, Y.J., Lei, Y., Shiling, A., 2016. Paleoenvironmental reconstruction of the late Santonian Songliao Paleo-lake. Palaeogeo. P. 457, 290–303.

Cheng, G.W., Wang, D.Q., Qin, L.G., Kong, Y.D., Yan, Q.K., Qin, G.T., 2002. Ecoenvironmental pretection of ecotourist development in Longji terraced landscape, Guangxi. J. Guilin Univ. Technol. 22, 94–98 (in Chinese with English abstract).

Ci, E., Yang, L.Z., Ma, L., Tang, Y.S., Cheng, Y.Q., Yin, S.X., 2007. Distribution and stable carbon isotope character of organic carbon of paddy soils with long-term

cultivation. J. Soil. Water. Conserv. 21, 72–75, 179 (in Chinese with English abstract).
Corrigan, D., Kloos, C., O'Connor, C.S., Timoney, R.F., 1973. Alkanes from four species of *Sphagnum* moss. Phytochem 12, 213–214.
Cranwell, P.A., 1973. Chain-length distribution of *n*-alkanes from lake sediments in relation to post-glacial environmental change. Freshw. Biol. 3, 259–265.
Cranwell, P.A., Eglinton, G., Robinson, N., 1987. Lipids of aquatic organisms as potential contributors to lacustrine sediments-II. Org. Geochem. 11, 513–527.
Cui, J.W., Huang, J.H., Pu, Y., Huang, X.Y., Xie, S.C., 2008. Comparison of lipid compositions between plant leaves and overlying soil in Heshang Cave, Qingjiang, Hubei Province and its significance. Quat. Sci. 28, 35–42 (in Chinese with English abstract).
Dar, R.A., Chandra, R., Romshoo, S.A., Lone, M.A., Ahmad, S.M., 2015. Isotopic and micromorphological studies of late quaternary loess–paleosol sequences of the Karewa Group: inferences for palaeoclimate of Kashmir valley. Quat. Int. 371, 122–134.
Deines, P., 1980. The isotopic composition of reduced organic carbon. In: Fritz, P., Fontes, J.C. (Eds.), Handbook of Environmental Isotope Geochemistry I, the Terrestrial Environment. Elsevier, Amsterdam, pp. 329–406.
Eglinton, G., Hamilton, R.J., 1967. Leaf epicuticular waxes. Science 156, 1322–1335.
Farquhar, G.D., Ehleringer, J.R., Hubick, K.T., 1989. Carbon isotope discrimination and photosynthesis. Annu. Rev. Plant. Biol. 40, 503–537.
Ferro-Vázquez, C., Martínez-Cortizas, A., Nóvoa-Muñoz, J.C., Ballesteros-Arias, P., Criado-Boado, F., 2014. 1500 years of soil use reconstructed from the chemical properties of a terraced soil sequence. Quat. Int. 346, 28–40.
Ficken, K.J., Li, B., Swain, D.L., Eglinton, G., 2000. An *n*-alkane proxy for the sedimentary input of submerged/floating freshwater aquatic macrophytes. Org. Geochem. 31, 745–749.
Gadot, Y., Davidovich, U., Avni, G., Avni, Y., Piasetzky, M., Faershtein, G., Golan, D., Porat, N., 2016. The formation of a mediterranean terraced landscape: mount Eitan, Judean highlands, Israel. J. Archaeol. Sci. Rep. 6, 397–417.
Gałka, M., Apolinarska, K., 2014. Climate change, vegetation development, and lake level fluctuations in Lake Purwin (NE Poland) during the last 8600 cal. BP based on a high-resolution plant macrofossil record and stable isotope data ($\delta^{13}C$ and $\delta^{18}O$). Quat. Int. 328–329, 213–225.
Ge, Q.S., Fang, X.Q., Wu, W.X., Zheng, J.Y., Hao, Z.X., He, F.N., Liu, H.L., Fu, H., 2011. Climate Change in Chinese Dynasties. Science Press, Beijing (in Chinese).
Gelpi, E., Schneider, H., Mann, J., Oró, J., 1970. Hydrocarbons of geochemical significance in microscopic algae. Phytochem 9, 603–612.
Gupta, N.S., Leng, Q., Yang, H., Cody, G.D., Fogel, M.L., Liu, W.G., Sun, G.P., 2013. Molecular preservation and bulk isotopic signals of ancient rice from the Neolithic Tianluoshan site, lower Yangtze River valley, China. Org. Geochem. 63, 85–93.
Hansen, J., Ruedy, R., Sato, M., Lo, K., 2010. Global surface temperature change. Rev. Geophys. 48, 1–29.
Henck, A., Taylor, J., Lu, H.L., Li, Y.X., Yang, Q.X., Crub, B., Breslow, S.J., Robbins, A., Elliott, A., Hinckley, T., Combs, J., Urgenson, L., Widder, S., Hu, X.X., Ma, Z.Y., Yuan, Y.W., Jian, D.J., Liao, X., Tang, Y., 2010. Anthropogenic hillslope terraces and swidden agriculture in Jiuzhaigou National Park, northern Sichuan, China. Quat. Res. 73, 201–207.
Huckleberry, G., Fadem, C., 2007. Environmental change recorded in sediments from the Marmes rockshelter archaeological site, southeastern Washington state, USA. Quat. Res. 67, 21–32.
Jiang, Y.J., Li, S.J., Cai, D.S., Chen, W., Liu, Y., Yu, Z., 2014. The genesis and paleoenvironmental records of Longji agricultural terraces, southern China: a pilot study of human-environment interaction. Quat. Int. 321, 12–21.
Li, S.J., Cai, D.S., Zhang, H.L., Shen, D.F., Zhao, X.G., Li, C.H., 2009. Environmental chnges record derived from sediment cores in Huixian Karst Wetlands, Guilin, China. J. Guangxi Norm. Univ. Nat. Sci. Ed. 27, 94–100 (in Chinese with English abstract).
Liu, Q., Liu, J.Q., Chen, X.Y., You, H.T., Chu, G.Q., Han, J.T., Mingram, J., Schettler, G., Negendank, J.F.W., 2005. Stable carbon isotope record of bulk organic matter from the Sihailongwan Maar Lake, Northeast China during the past 18.5 ka. Quat. Sci. 25, 711–721 (in Chinese with English abstract).
Liu, W.G., Huang, Y.S., An, Z.S., Clemens, S.C., Li, L., Prell, W.L., Ning, Y.F., 2005. Summer monsoon intensity controls C_4/C_3 plant abundance during the last 35 ka in the Chinese Loess Plateau: carbon isotope evidence from bulk organic matter and individual leaf waxes. Palaeogeo. P. 220, 243–254.
Ni, Z.Y., Yang, G.F., Huang, J.H., Zhang, X.J., Cheng, J., Yin, G.M., 2011. Organic carbon isotopic characteristics of Beijing Plain since Late Pleistocene and their paleoenvironmental implications. Acta. Geosci. Sin. 32, 171–177 (in Chinese with English abstract).
O'Beirne, M.D., Strzok, L.J., Werne, J.P., Johnson, T.C., Hecky, R.E., 2015. Anthropogenic influences on the sedimentary geochemical record in western Lake Superior (1800–present). J. Gr. Lakes 41, 20–29.
Osmond, C.B., 1978. Crassulacean acid metabolism: a curiosity in context. Annu. Rev. Plant. Physiol. 29, 379–414.
Parker, A.G., Lee-Thorp, J., Mitchell, P.J., 2011. Late Holocene Neoglacial conditions from the Lesotho highlands, southern Africa: phytolith and stable carbon isotope evidence from the archaeological site of Likoaeng. P. Geol. Assoc. 122, 201–211.
Pu, Y., Zhang, H.C., Wang, Y.L., Lei, G.L., Nace, T., Zhang, S.P., 2011. Climatic and environmental implications from *n*-alkanes in glacially eroded lake sediments in Tibetan Plateau: an example from Ximen Co. Chin. Sci. Bull. 56, 1503–1510.
Puy, A., Balbo, A.L., 2013. The genesis of irrigated terraces in al-Andalus. A geoarchaeological perspective on intensive agriculture in semi-arid environments (Ricote, Murcia, Spain). J. Arid. Env. 89, 45–56.
Rao, Z.G., Zhu, Z.Y., Jia, G.D., Chen, F.H., Barton, L., Zhang, J.W., Qiang, M.R., 2010. Relationship between climatic conditions and the relative abundance o modern C_3 and C_4 plants in three regions around the North Pacific. Chin. Sci. Bull. 55, 1931–1936.
Rao, Z.G., Xu, Y.B., Xia, D.S., Xie, L.H., Chen, F.H., 2013. Variation and paleoclimatic significance of organic carbon isotopes of Ili loess in arid Central Asia. Org. Geochem. 63, 56–63.
Ratnayake, N.P., Suzuki, N., Okada, M., Takagi, M., 2006. The variations of stable carbon isotope ratio of land plant-derived *n*-alkanes in deep-sea sediments from the Bering Sea and the North Pacific Ocean during the last 250,000 years. Chem. Geol. 228, 197–208.
Reimer, P.J., Baillie, M.G.L., Bard, E., Bayliss, A., Beck, J.W., Blackwell, P.G., Bronk Ramsey, C., Bulk, C.E., Burr, G.S., Edwards, R.L., Friedrich, M., Grootes, P.M., Guilderson, T.P., Hajdas, I., Heaton, T.J., Hogg, A.G., Hughen, K.A., Kaiser, K.F., Kromer, B., McCormac, F.G., Manning, S.W., Reimer, R.W., Richards, D.A., Southon, J.R., Talamo, S., Turney, C.S.M., van der Plicht, J., Weyhenmeyer, C.E., 2009. IntCal09 and Marine09 radiocarbon age calibration curves, 0-50,000 years cal BP. Radiocarbon 51, 1111–1150.
Schäfer, I.K., Bliedtner, M., Wolf, D., Faust, D., Zech, R., 2016. Evidence for humid conditions during the last glacial from leaf wax patterns in the loess–paleosol sequence El Paraíso, Central Spain. Quat. Int. 407, 64–73.
Selvaraj, K., Wei, K.Y., Liu, K.K., Kao, S.J., 2012. Late Holocene monsoon climate of northeastern Taiwan inferred from elemental (C, N) and isotopic ($\delta^{13}C$, $\delta^{15}N$) data in lake sediments. Quat. Sci. R 37, 48–60.
Tong, Q.M., 2006. The common properties of three ancient terraces and the unique properties of Ziquejie Terrace in China. Land Resour. Her. 3, 73–74 (in Chinese).
Trombold, C.D., Israde-Alcantara, I., 2005. Paleoenvironment and plant cultivation on terraces at La Quemada, Zacatecas, Mexico: the pollen, phytolith anddiatom evidence. J. Archaeol. Sci. 32, 341–353.
van Bree, L.G.J., Rijpstra, W.I.C., Cocquyt, C., Al-Dhabi, N.A., Verschuren, D., Sinninghe Damsté, J.S., de Leeuw, J.W., 2014. Origin and palaeoenvironmental significance of C_{25} and C_{27} *n*-alk-1-enes in a 25,000-year lake-sedimentary record from equatorial East Africa. Geochim. Cos. A 145, 89–102.
Wang, J.J., 2007. Research of the Relationship between Climatic Changes and Wars in Chinese History. Master Thesis. Zhejiang Normal University, China (in Chinese with English abstract).
Wang, S.W., Cai, J.N., Zhu, J.H., Gong, D.Y., 2002. The interdecadal variations of annual precipitation in China during 1880's –1990's. Acta. Meteorol. Sin. 60, 637–639 (in Chinese with English abstract).
Wang, S.W., Tang, G.L., 2011. Observed climate change. In: Qin, D.H. (Ed.), National Assessment Report of Climate Change. Science Press, Beijing, pp. 38–42 (in Chinese).
Wang, S.W., Ye, J.L., Gong, D.Y., 1998. Climate in China during the little Ice age. Quat. Sci. 1, 54–64 (in Chinese with English abstract).
Xi, C.F., 1994. Soil Taxonomy. China Agriculture Press, Beijing (in Chinese).
Xie, S.C., Liang, B., Guo, J.Q., Yi, Y., Evershed, R.P., Maddy, D., Chambers, F.M., 2003. Biomarkers and the related global change. Quat. Sci. 23, 521–528 (in Chinese with English abstract).
Zech, M., Rass, S., Buggle, B., Löscher, M., Zöller, L., 2012. Reconstruction of the late Quaternary paleoenvironments of the Nussloch loess paleosol sequence, Germany, using *n*-alkane biomarkers. Quat. Res. 78, 226–235.
Zhang, D.E., 1980. Characteristics of winter temperature changes during the past 500 years in southern China. Chin. Sci. Bull. 6, 270–272 (in Chinese).
Zhang, Z.H., Zhao, M.X., Eglinton, G., Lu, H.Y., Huang, C.Y., 2006. Leaf wax lipids as paleovegetational and paleoenvironmental proxies for the Chinese Loess Plateau over the last 170 kyr. Quat. Sci. R 25, 575–594.
Zheng, J.Y., Wang, W.C., Ge, Q.S., Man, Z.M., Zhang, P.Y., 2006. Precipitation variability and extreme events in Eastern China during the past 1500 years. Terr. Atmos. Ocean. Sci. 17, 579–592.
Zheng, Y.H., Cheng, P., Zhou, W.J., 2005. Paleo-vegetation and paleo-climate *n*-alkanes and compound-specific carbon isotopic compositions. Mar. Geol. Quat. Geol. 25, 99–104 (in Chinese with English abstract).
Zou, S.L., Zhu, J.Y., Xiong, B.S., Li, R.C., Jin, F., Xie, S.C., 2007. Distribution of *n*-alkanes as indicators of paleovegetation change in ancient cultural layers of Jinluojia site in Macheng, Hubei Province. Mar. Geol. Quat. Geol. 27, 119–125 (in Chinese with English abstract).